

## Nuclear Scattering of 50- to 130-Mev $\gamma$ Rays\*

GEORGE E. PUGH,<sup>†</sup> RICARDO GOMEZ,<sup>‡</sup> DAVID H. FRISCH, AND G. SARGENT JANES<sup>§</sup>

*Department of Physics and Laboratory for Nuclear Science, Massachusetts Institute of Technology, Cambridge, Massachusetts*

(Received July 12, 1956)

Using targets of H, D, Li, Be, C, Cu, and Sn, we have measured the energy distribution of scattered  $\gamma$  rays at 45°, 90°, and 135°. In first approximation one would expect a scattering cross section given by the coherent addition of Thomson scattering amplitudes for  $Z$  free protons. Important deviations, probably of mesonic origin, are observed above 90 Mev. Below 70 Mev in complex nuclei there is an increase in cross section which probably results from nuclear resonance scattering. At small angles in the forward direction, we observe large numbers of inelastically scattered  $\gamma$  rays, which apparently result from inner bremsstrahlung associated with electron pair production.

### I. INTRODUCTION

SCATTERING of x-rays by electrons has had two main objects: (a) the study of the interaction between free electrons and the electromagnetic field, thus checking the validity of Dirac's equation in the region of experimentation, (b) the study of the electronic structure of complex systems, i.e., atoms, molecules, crystals, etc.<sup>1</sup> The scattering by complex systems can in fact yield information of both types (a) and (b), and in particular it can separate the spin-dependent from the non-spin-dependent parts of the single-particle cross section, which are difficult to separate by observing the scattering by free particles.

Scattering of  $\gamma$  rays by complex nuclei and by hydrogen has parallel objectives: (a) the understanding of the interaction between the electromagnetic field and the free nucleons, (b) the study of nuclear structure. For the purpose of comparison, we will review briefly the findings of the atomic x-ray scattering.

The scattering of a photon by a free electron is given by the Klein-Nishina equation. When  $Z$  electrons are grouped together in an atom their scattering depends also on the momentum transferred in the scattering,  $\hbar(\Delta k)$ , and the radius of the atom,  $a$ . In the high-energy, short-wavelength limit, when  $a(\Delta k) \gg 1$ , the scattering cross section is the incoherent sum of the Klein-Nishina cross sections for  $Z$  free electrons with the velocity distribution they have in the atom. As we decrease the photon energy (or decrease the scattering angle) so that  $(\Delta k)$  decreases, elastic coherent scattering from the whole assemblage (Rayleigh) becomes important, standing in the approximate ratio<sup>1</sup>  $Z^2 f^2 \sigma_T / [Z(1-f^2)\sigma_{KN}]$

to the inelastic scattering. Here

$$f = \frac{1}{Z} \int \psi^*(x_1, x_2, \dots) \sum_{i=1}^{i=Z} \exp(-i\Delta k \cdot \mathbf{x}_i) \times \psi(x_1, x_2, \dots) dx_1^3 dx_2^3 \dots$$

is the atomic form factor,  $\sigma_T = \frac{1}{2}(e^2/Mc^2)^2(1+\cos^2\theta)$  the Thomson cross section, and  $\sigma_{KN}$  the Klein-Nishina cross section. When  $(\Delta k)a \ll 1$ , the scattering cross section approaches zero for a neutral atom, but for an ion approaches the Thomson value  $\frac{1}{2}(Z'e^2/M'c^2)^2 \times (1+\cos^2\theta)$  for an object with net charge  $Z'e$  and total mass  $M'$ .

The scattering of photons by nucleons differs from x-ray scattering by electrons in two important respects: First, the order of magnitude of the scattering cross section is smaller by  $(m/M)^2 \approx 3 \times 10^{-7}$ , where  $m$  is the electron mass and  $M$  the nucleon mass. Second, although nucleons have spin  $\frac{1}{2}$ , their structure gives rise to their anomalous magnetic moments and probably to other electromagnetic effects which will affect the scattering, so that the Klein-Nishina cross section should be correct only in the low-energy limit.

For complex nuclei at very low energies the cross section should be the Thomson value for a rigid body of charge  $Ze$  and mass  $AM$ ,

$$d\sigma = \frac{1}{2}[(Ze)^2/AMc^2]^2(1+\cos^2\theta)d\Omega.$$

In a region around 20 Mev, where the  $\gamma$ -ray energy is comparable with the nuclear binding energy, the scattering cross section becomes quite large because of the contribution of nuclear resonance scattering.

As the energy becomes large compared with the nuclear binding energy, the nuclear resonance scattering decreases and one expects the scattering amplitude from individual protons in the nucleus to approach the free-particle limit. It can be shown<sup>2</sup> that the amplitude for elastic scattering by nuclei, for energies between 80 and 150 Mev, approaches the Thomson value despite the anomalous magnetic moments of proton and neutron, if one neglects the dispersive scattering which should be associated with the photoproduction of

\* This work was supported in part by the joint program of the U. S. Atomic Energy Commission and the Office of Naval Research.

<sup>†</sup> Now at "Institute for Defense Analyses," Pentagon, Washington 25, D. C.

<sup>‡</sup> Now at California Institute of Technology, Pasadena, California.

<sup>§</sup> Now at Research Laboratories, AVCO Manufacturing Company, Everett, Massachusetts.

<sup>1</sup> A. H. Compton and S. K. Allison, *X-Rays in Theory and Experiment* (D. Van Nostrand Company, Inc., New York, 1935).

<sup>2</sup> R. Gomez, Ph.D. thesis, Massachusetts Institute of Technology, 1956 (unpublished).

mesons. The cross section is given in this case by

$$\sigma_{\text{elastic}} = Z^2 f^2(\Delta k) \sigma_{\pi},$$

where  $f(\Delta k)$  is the form factor for the nuclear charge distribution, analogous to the atomic form factor.

Any large deviation of the elastic scattering from the formula above has to be attributed to the internal structure of nucleons. Such deviations are expected because  $\gamma$  rays are known to interact with nucleons, producing  $\pi$  mesons in large numbers. Gell-Mann *et al.*<sup>3</sup> have shown by means of very general relations that the scattering cross section at  $0^\circ$  can be related to the total absorption cross section if this is known for all energies. They find, for example, that at meson threshold, around 135 Mev in the c.m. system, the scattering cross section at  $0^\circ$  for protons should be close to zero. Assuming specific models which agree with the data on photomeson production, it is possible to predict the scattering at all angles.

The study of this mesonic "polarizability" is the main object of the experiment reported on this paper.

The very small cross section ( $\approx 10^{-31}$  cm<sup>2</sup>) makes nuclear  $\gamma$ -ray scattering experiments quite difficult. In the energy region below 2 Mev it is almost a hopeless task to observe nuclear scattering because of the very large scattering by atomic electrons. From 2 to 5 Mev it is still quite difficult but a subtraction is possible. Above 10 Mev and at angles greater than  $30^\circ$ , the collusive momentum in scattering is large enough so that the elastic (Rayleigh) scattering by the electron cloud becomes very small.<sup>4</sup> The Compton scattering<sup>5</sup> by electrons is still appreciable, but owing to the great energy degradation suffered by the scattered photon it can easily be distinguished from a photon scattered by a nucleon.

Nuclear scattering has been observed by Burkhardt<sup>6</sup> in the region from 1 to 3 Mev. Scattering by the giant dipole resonance<sup>7</sup> was first observed by Dressel *et al.*,<sup>8</sup> and Stearns.<sup>9</sup> Fuller and Hayward<sup>10</sup> have done extensive work in the region from 4 to 28 Mev at  $120^\circ$  for elements heavier than Cu. They have been able to resolve the giant resonance into two peaks, one at the neutron threshold and the other at around 16 Mev. The existence of these two peaks was first predicted by Bethe and Ashkin.<sup>11</sup>

Above 50 Mev, nuclear scattering was first observed

<sup>3</sup> Gell-Mann, Goldberger, and Thirring, Phys. Rev. **95**, 1612 (1954).

<sup>4</sup> Raman scattering is always negligible at energies higher than 1 kev.

<sup>5</sup> The scattering in which one electron is left in an inbound state.

<sup>6</sup> J. Burkhardt, Phys. Rev. **100**, 192 (1955).

<sup>7</sup> M. Goldhaber and E. Teller, Phys. Rev. **74**, 1046 (1948).

<sup>8</sup> Dressel, Goldhaber, and Hanson, Phys. Rev. **77**, 754 (1950).

<sup>9</sup> M. B. Stearns, Phys. Rev. **87**, 706 (1952).

<sup>10</sup> E. G. Fuller and E. Hayward, Phys. Rev. **95**, 1106 (1954).

<sup>11</sup> H. A. Bethe and J. Ashkin, *Experimental Nuclear Physics*, edited by E. Segrè (John Wiley and Sons, Inc., New York, 1953), Vol. 1, p. 347.

by three of the authors<sup>12</sup> in a preliminary experiment on various elements from Li to Pb, at  $90^\circ$  and  $135^\circ$ . Recently Oxley and Telegdi<sup>13</sup> have measured the  $H_2$  cross section integrated from 25 to 95 Mev at different angles; their results seem to be in good agreement with the Klein-Nishina cross section except at angles smaller than  $45^\circ$ .

This paper describes an experiment which is an extension of the one described in our preliminary report.<sup>12</sup> However, the reliability of the equipment and its calibration have been greatly improved.

Photons of energies between 50 and 130 Mev were scattered by nuclei of various elements and the work was extended to include measurements at  $45^\circ$  in addition to  $90^\circ$  and  $135^\circ$ . The work has also been extended to include data on hydrogen and deuterium. The upper limit of  $\gamma$ -ray energy was chosen below the  $\pi^0$  photoproduction threshold; otherwise photons resulting from the decay of  $\pi^0$  mesons would have been confused with the scattered photons. The lower energy limit was set by the decreased sensitivity and resolution of the detector which was chosen primarily for its properties at the high energies. The range of angles was limited both by the detector geometry and, in the forward direction, by a large number of photons probably resulting from radiative pair production.

At the low energies, between 50 and 80 Mev, the binding of the nucleon in the nucleus shows up as an increased scattering, probably associated with electric dipole resonances in the nucleus.<sup>7,10</sup> As expected, no such increase in scattering was observed for hydrogen.

Above 80 Mev, the scattering observed in this experiment can be interpreted as coming from essentially free protons and neutrons in nuclei of uniform density and radius  $R = 1.2A^{1/3} \times 10^{-13}$  cm, provided one includes the mesonic polarizability of the nucleons.

## II. EXPERIMENT

### A. General Discussion

These experiments were conducted in the bremsstrahlung beam of the MIT ONR Synchrotron (Fig. 1). The maximum beam energy was held between 129 and 132 Mev, which is just below the threshold for  $\pi^0$  photoproduction. Consequently, there were no  $\gamma$  rays from  $\pi^0$  decays which might otherwise have been mistaken for scattered  $\gamma$  rays. The energy distribution of scattered  $\gamma$  rays was measured (using an energy sensitive counter with an effective energy resolution of about 15 percent), and was compared with the energy distribution in the incident beam. No attempt was made to observe recoil particles, or to measure the energy of individual  $\gamma$  rays before scattering. Hence both elastic and inelastic events were accepted and were recorded, not in their initial energy groups, but in

<sup>12</sup> Pugh, Frisch, and Gomez, Phys. Rev. **95**, 590 (1954).

<sup>13</sup> C. L. Oxley and V. L. Telegdi, Phys. Rev. **100**, 435 (1955).

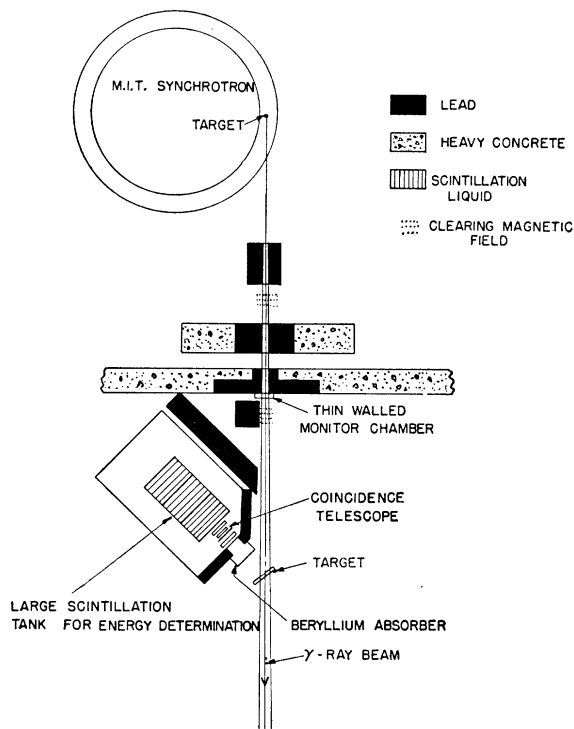


FIG. 1. Plan view of experiment.

their final energy groups after scattering. For most of our work the inelastic scattering is expected to be small, but an accurate interpretation of the data requires an estimate of the inelastic scattering.

The cross section for nuclear  $\gamma$ -ray scattering is small relative to photo nuclear reactions which are ordinarily observed. Differential cross sections range from 10 millimicrobarns ( $10^{-32}$  cm<sup>2</sup>) for hydrogen to 80 microbarns for lead. The available beam intensity at the MIT ONR Synchrotron seldom exceeded  $5 \times 10^7$  equivalent quanta/sec. Consequently the experiment was carried out using rather thick targets, up to 0.25 radiation length, and a large solid angle ( $\sim 0.1$  steradian). The counting rate ranged from 7 real events per hour with hydrogen to about 2 events per minute with heavier nuclei.

Data were taken over a six month period. During most of the time the equipment was operated 24 hours a day. Typical runs were about 24 hours for one element at one angle. The beryllium data took about ten days of running time. The data on hydrogen required about two weeks per angle.

### B. $\gamma$ -Ray Source

The  $\gamma$ -ray beam is produced when electrons in the synchrotron, having reached their peak energy, are allowed to spiral in and strike an internal tungsten target. The magnetic field is so adjusted that an electron which strikes the target at peak field has an energy

about 2 Mev less than the  $\pi^0$  rest mass. The peak machine energy was calibrated by integrating the voltage induced in a carefully measured wire loop in the orbit gap of the machine. This loop, which was varnished to the vacuum doughnut, was one inch wide and completely encircled the machine both above and below the electron orbit at the target radius. The energy calibration was also checked within a few Mev by measuring the peak energy of positrons produced in the beam. The machine energy was monitored regularly using both the voltage on the condenser bank and an electronic integrator on another wire loop.

The duration of the  $\gamma$ -ray burst is controlled by turning off the rf oscillator very slowly. During most of the experiment the oscillator was adjusted to stretch the beam out over a period of about 800 sec. This gave an energy spread between 129 and 132 Mev.

During regular experimental runs the beam was monitored simultaneously by a thin-walled ionization chamber just behind the collimator and by a thick-walled chamber in front of a backstop at the far end of the room. Both chambers operated electronic integrators from which we read our total exposures. Both monitors were checked periodically against a standard thick-walled ionization chamber which discharged a low-leakage condenser whose voltage was read by a Victoreen type electrostatic voltmeter. The standard ionization chamber had been previously calibrated against the Illinois calorimetric standard but as will be pointed out, this calibration is not used in calculating our absolute cross sections.

### C. Targets

Targets were placed so as to intercept the entire beam. Thin targets were placed to bisect the angle between the incident and scattered beam, while targets whose thickness was comparable to or larger than the beam diameter were placed perpendicular to the beam. Appropriate corrections in the effective solid angle and self-absorption were computed for each geometry.

The maximum tolerable target thickness which could be used without serious trouble from multiple events in the target was obtained experimentally. Large-angle multiple events which might spuriously increase the counting rate are most likely to arise from low-energy  $\gamma$  rays, for which the counting rates are comparatively high. Hence a short run was usually sufficient to determine the allowable target thickness. The regular targets used ranged from 0.25 radiation length at  $135^\circ$  to 0.04 radiation length at  $45^\circ$ . Targets as thin as 0.01 radiation length were used to test for multiple events in small-angle data. For runs which were particularly sensitive to background the targets were put in a helium atmosphere to reduce atmospheric scattering, and a clearing magnet was placed after the last collimator to remove charged contaminants from the beam. The target-out counting rate was negligible in

all cases except for hydrogen, where a careful subtraction had to be made for background from the empty container, which constituted between 30% and 50% of the total counting rate.

The hydrogen target<sup>14</sup> consisted of a 5-inch high, 4-inch diameter cylindrical container in an evacuated chamber. The container, which could be used for hydrogen or deuterium, was refrigerated using cold He gas from a liquid helium Dewar.

During the early stages of the experiment the target was in a preliminary state of design and the hydrogen was surrounded by a two-layer wall totaling 6 mils of beryllium copper. This was later reduced to 3 mils and finally, for the work at 45°, to a single wall amounting to just 0.7 mil of stainless steel.

#### D. Detectors

Figure 2 shows a close-up of the detecting apparatus. In this sketch the incident beam striking the target is perpendicular to the page. Scattered  $\gamma$  rays from the target pass through a six-inch beryllium absorber and are detected by a conventional  $\gamma$ -ray telescope, consisting of an anticoincidence counter *A*, a  $\frac{1}{2}$ -radiation-length lead converter, and two coincidence counters, *B* and *C*. The electron pair from the converter then enters a large glass tank of scintillation liquid *D*, which estimates the energy of the  $\gamma$  ray by measuring the ionization loss in the liquid. The tank is completely painted on the inside with an emulsion of  $\text{TiO}_2$  in waterglass except for clear spaces where 12 phototube light pipes are attached on the outside. The chief uncertainty in this energy determination arises from  $\gamma$  rays radiated by members of the electron pair which can pass undetected out the back of the counter.

An event occurring in the large counter (*D*) is recorded by a 9-channel pulse-height analyzer whenever it occurs in coincidence with events in *B* and *C* and no event is recorded by counter *A*. The bias in counters *B* and *C* is set to respond to all events showing at least twice minimum ionization in the counters.

Determination of the scattered  $\gamma$ -ray energies depends entirely on the analysis of pulse heights obtained from photomultipliers. Hence, it was essential to maintain a constant ratio between ionization losses and pulse height. It was found that the pulse-height distribution of cosmic ray traversals in the large counter provided a very convenient standard for comparison. Indeed, about a two-minute run (without looking for coincidences in the other counters) on cosmic-ray traversals of the large counter enabled us to estimate the over-all gain to about 1 percent. Thermal variation in scintillator efficiency was probably the largest single factor producing pulse-height drift in the equipment. The worst drifts were of the order of a few percent per day and could be corrected easily.

<sup>14</sup> Janes, Hyman, and Strumski, Rev. Sci. Instr. (to be published).

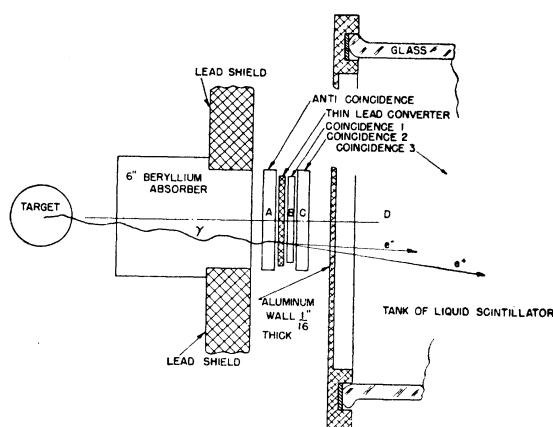


FIG. 2. Close-up of detectors.

#### E. Background

In most respects the experiment was remarkably free of serious background problems. Targets were always chosen sufficiently thin so that multiple events in the target formed a negligible fraction of the total. In the case of hydrogen and deuterium it was necessary to subtract scattering by the empty container, but in all other cases the target-out background was completely negligible.

Care was necessary to be sure that all target associated events were indeed scattered  $\gamma$  rays. Heavy-particle charged events were ruled out by the Be absorber, which was thick enough to stop the most energetic available protons.

The absorber also stopped low-energy electron events. Remaining electrons were screened out, first by the anticoincidence which was about 98% efficient and second by the double electron bias in the coincidence crystals.

Neutron background is a common difficulty in  $\gamma$ -ray experiments, but there was no evidence that neutrons contributed significantly to the counting rate. Attenuation of the counting rate with lead absorbers was as expected for a pure  $\gamma$ -ray beam. The use of a neutron-equivalent aluminum converter gave only the counting rate to be expected from its  $\gamma$ -ray conversion coefficient. Furthermore, a pulse-height analysis of accepted events in the coincidence crystals showed no indication of a large pulse-height group that might correspond to knock-on protons.

By taking the data as a difference between converter-in and converter-out counting rates we required that the conversion occur in the lead converter.

Accidental events were apparently no serious problem, because the introduction of an appropriate delay in any signal from the coincidence telescope stopped the counting rate almost completely. There were, however, difficulties due to the accidental anticoincidence of real  $\gamma$  rays. Because the bias on the anticoincidence counter

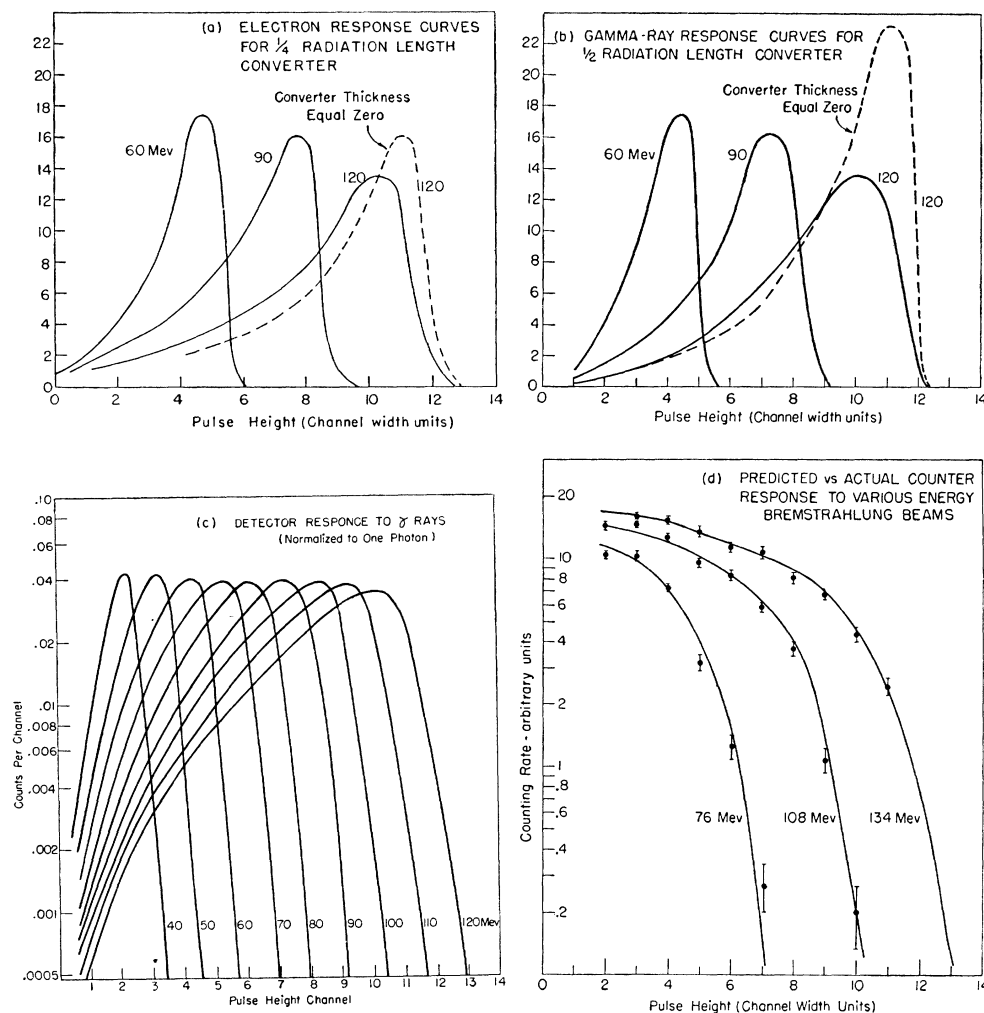


FIG. 3. Response curves for the counter.

was set to respond to all single minimum events the counting rate in this crystal was often very large. This effect was normally less than 3% but a 20% correction was required in the case of hydrogen at 45°. The size of this correction was determined by measuring the fraction of time the anticoincidence was in effect.<sup>2</sup>

In cases where a careful comparison was required between scattering at different angles or between elements, the data were taken in alternating order to eliminate any effects from changes in beam intensity or equipment stability. There was no indication that this precaution was necessary.

#### F. Calibration and Absolute Normalization

The accuracy of our results, especially with regard to the energy dependence of the cross section, is dependent on a prior understanding of the pulse-height response of the large tank *D*. This response (for centrally incident  $\gamma$  rays) was studied experimentally in considerable detail. Corrections to the central response

for off-axis and diagonally incident  $\gamma$  rays were made by comparing the central and off-axis response for a 1/2-cm-diameter bremsstrahlung beam of different peak energies. For our actual experimental geometries, the largest correction occurred at large pulse heights and did not exceed 20% in counting rate.

Because we do not have a source of monoenergetic  $\gamma$  rays in this energy region, the central response of the counter was first obtained using a beam of magnetically analyzed monoenergetic electrons. The electrons, produced in a converter in the bremsstrahlung beam, were counted before entering the counter so that both the absolute efficiency and pulse height response could be measured. The absolute efficiency is especially important for low-energy electrons where scattering or radiation in the converter and coincidence crystals can result in failure to obtain the required coincidence. Response curves [Fig. 3(a)] were taken for three different thicknesses of the converter using electrons of 12 different energies. From these data and the known  $\gamma$ -ray to electron-pair cross sections, it is possible to

predict the response to incident  $\gamma$  rays [Fig. 3(b)]. For instance, if  $P(E, X, h)$  is the probability of obtaining a pulse height  $h$  from an electron of energy  $E$  which is incident on a converter of thickness  $X$ , then the pulse height response  $P'(E_\gamma, E, X, h)$  to be expected from a  $\gamma$  ray of energy  $E_\gamma$  which splits into electrons of energy  $E$  and  $E_\gamma - E$  at a distance  $X$  from the back of the converter is given by

$$P'(E_\gamma, E, X, h) = \int P(E, X, h') P(E_\gamma - E, X, h - h') dh'.$$

These integrations were carried out numerically and for normalization the resulting curves were multiplied by the probability that a  $\gamma$  ray of energy  $E_\gamma$  would materialize as indicated. The sum of normalized response curves for all possible ways of materialization in the actual converter gives the final response curve  $R(E_\gamma, h)$ . The complete set of curves  $R(E_\gamma, h)$  which were actually used are shown in Fig. 3(c). These curves can be appropriately weighted to predict the response to a bremsstrahlung beam. The predicted response for an axially incident bremsstrahlung beam was checked experimentally for several peak energies using a narrow beam of  $\gamma$  rays from the synchrotron. This comparison is shown in Fig. 3(d).

The pulse-height comparison is excellent but the counter showed about a 10% higher counting rate than expected. This discrepancy in absolute normalization has been arbitrarily removed in the comparison. The discrepancy could come from a number of sources including the absolute normalization of the beam intensity. However, we suspect that the most likely cause is a bias problem in the coincidence crystals.

The bias is set to include almost all double minimum events, but because of Landau fluctuations in ionization one inevitably includes some of those events in which only one electron of the pair penetrates both coincidence crystals. (This difficulty is of course aggravated by any nonuniformities in the crystal response.) Single electron events of this type are not included in the prediction obtained from the electron calibration. Experimentally we find that when all single minimum events are included the counting rate increases by about 40%.

We need to know the pulse-height response of the counter in order to interpret the scattering cross section as a function of energy, but we do not need to know either the absolute beam intensity or the absolute detection efficiency of the counter. The experimentally important quantity is the ratio, in each energy interval, between the number of  $\gamma$  rays in the incident and scattered beams. This comparison is obtained by placing the counter directly in the bremsstrahlung beam. However, to obtain useful data one must scale the beam intensity down by about a factor of  $10^5$  from an intensity which can be recorded directly by our monitor to an intensity which can be handled by our counter.

In this way, the uncertainty in the scale factor becomes the only real uncertainty in the absolute normalization. This scaling was carried out using counters for a factor of 50 and ionization chambers for about a factor of 2000. All comparisons were extrapolated to zero intensity in order to eliminate rate-dependent effects. The total error in the scale factor is probably less than  $\pm 7\%$ .

### G. Analysis of the Data

In an actual experiment,  $n(E_s)dE_s$ , the number of scattered  $\gamma$  rays in the interval  $dE_s$  of mean energy  $E_s$  incident on the converter, is connected to the observed pulse-height distribution  $N(h)dh$  by the relation

$$N(h) = \int_{E_s} n(E_s) R(E_s, h) dE_s,$$

where  $R(E_s, h)$  is the pulse-height response of the counter, described in the previous section. More than half the  $\gamma$  rays falling in any pulse-height channel come from within a 15-Mev interval. This narrow response is obtained despite the apparently broad response curves  $R(E_s, h)$ . It is due to a combination of a counter response which is sharp on the high pulse-height side and a counting rate which is a rapidly falling function of energy. In this way, for any given channel, the lower energy photons do not contribute, and there are so few photons of higher energy that their contribution is quite small. Each experimental point has an effective energy width between 10 and 15 Mev, and the statistical errors shown are those of the corresponding pulse-height channels.

## III. RESULTS

### A. Hydrogen

For hydrogen and deuterium we have plotted the ratio between the observed yield of scattered  $\gamma$  rays per steradian and the expected yield based on the Klein-Nishina cross section for a particle of protonic mass. For the purpose of this discussion we have also indicated the ratio  $\sigma_P/\sigma_{KN}$  (dashed line).  $\sigma_P$  is the Klein-Nishina cross section as modified by Powell<sup>15</sup> to include the proton anomalous magnetic moment.

The statistical errors are sufficiently large that the points at  $90^\circ$  and  $135^\circ$  [Fig. 4 (a) and (b)] could fit either  $\sigma_P$  or  $\sigma_{KN}$ . At  $45^\circ$  [Fig. 4(c)] the observed yields do not agree with either theory. Below 80 Mev there is an excess yield which is probably not of nuclear origin, but appears to be associated with radiative pair production. This will be discussed later, together with the results from complex nuclei. Above 100 Mev the data suggest rather strongly that the cross section is less than either  $\sigma_P$  or  $\sigma_{KN}$ . There are several reasons to believe this drop is real: (1) At forward angles experimental error would be likely to increase rather than

<sup>15</sup> J. L. Powell, Phys. Rev. **75**, 32 (1949).

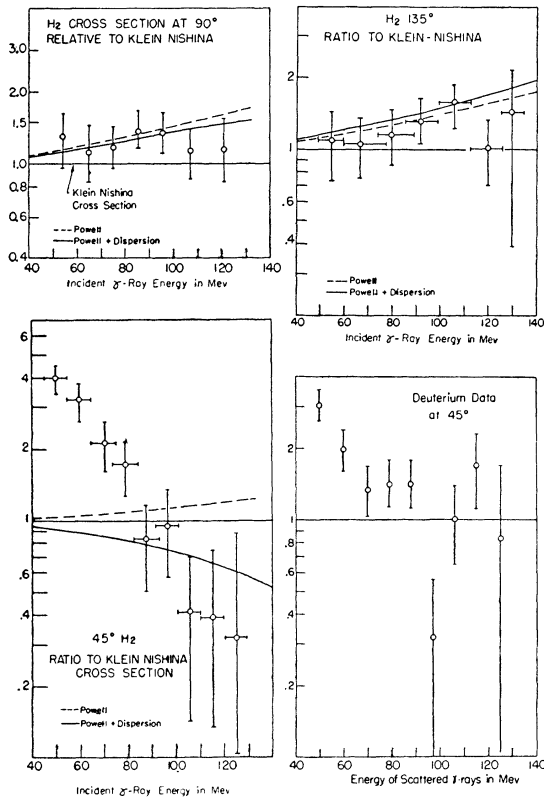


FIG. 4.  $\gamma$ -ray scattering by hydrogen and deuterium.

decrease observed yields. (2) The data for complex nuclei show a similar drop. (3) Theoretically, Gell-Mann and Goldberger<sup>16</sup> have used meson photoproduction data to show by means of dispersion relations that the scattering cross section at  $0^\circ$  should be very small near meson threshold. Thus it is not surprising to see a decrease in the  $45^\circ$  cross section in the energy range from 100 to 135 Mev.

Less time was spent in obtaining the deuterium data [Fig. 4(d)] and the statistics on it are quite poor.

### B. Complex Nuclei

The data obtained with complex nuclei are displayed in Fig. 5. To allow a convenient comparison between elements, we have plotted the ratio between the observed number of scattered  $\gamma$  rays in each energy interval and the number expected on the basis of an energy-independent cross section given by  $Z^2(e^2/Mc^2)^2 \times (1 + \cos^2\theta)$ . This cross section corresponds to the Thomson scattering one would expect from  $Z$  free protons in a point nucleus.

As we have previously remarked, because of the finite nuclear size the elastic scattering should be reduced by the form factor  $f^2(\Delta k \cdot R)$ . As an aid in evaluating the

<sup>16</sup> M. Gell-Mann and M. L. Goldberger, *Proceedings of the 1954 Glasgow Conference on Nuclear and Meson Physics* (Pergamon Press, London, 1955).

data we have plotted the form factor, the light line in each graph, for a uniform spherical nucleus of radius  $1.2A^{1/3} \times 10^{-13}$  cm. For comparison with the heavier elements, where the result is strongly affected by nuclear radius, we have plotted the form factors for two other radii. The plotted form factors are essentially independent of detailed nuclear shape. The form factor becomes strongly shape-dependent only for large momentum transfers where the elastic scattering is a small fraction of the total.

In this experiment one expects to find a certain amount of inelastic scattering superimposed on the elastic scattering. If we use a simple approximation inherited from atomic x-ray scattering, then the cross section for this inelastic scattering would be  $(1-f^2)\sigma_{KN}$ .<sup>1</sup> The heavy line above each of the form factor curves indicates how much the observed result would be increased by the addition of these inelastic events. This line was calculated allowing for both the Compton degradation of scattered  $\gamma$  rays and the momentum spread of protons in the nucleus.

The inelastic scattering is quite sensitive to nucleon-nucleon correlations in the nucleus. The  $(1-f^2)$  approximation, which is correct only in the case of zero correlation, is probably a much worse estimate for nuclei than for the atomic case. Even the correlation introduced by the exclusion principle can have an important effect, because many appropriate final states are occupied. A rough calculation suggests that about half the inelastic scattering implied by the  $(1-f^2)$  will not occur because of the exclusion principle. On the other hand, if we make the reasonable assumption that we should use the Powell cross section instead of  $\sigma_{KN}$  and secondly include an additional Powell-type cross section for the neutrons, we might regain most of that factor of two.

In any case the inelastic scattering is a fairly small correction, and for the purpose of the following discussion we shall use elastic scattering plus  $(1-f^2)$  as a reference cross section, indicated by the heavy lines in Fig. 5. It will be referred to as the *modified Thomson yield*. We shall now proceed to discuss the data by comparing the experimental points with the modified Thomson yields shown in Fig. 5.

#### 1. 50 to 90 Mev

In the region from 50 to 90 Mev the observed yields are larger at  $90^\circ$  and  $135^\circ$  and much larger at  $45^\circ$  than the modified Thomson yields.

In complex elements one expects scattering from the excited states of the nucleus. Such scattering is predominantly electric dipole and would be expected to have the same angular dependence as the Thomson scattering. At  $90^\circ$  and  $135^\circ$  the excess yield is proportional to the Thomson and can probably be attributed to this resonance scattering. A comparison was made of our low-energy results on copper with those obtained

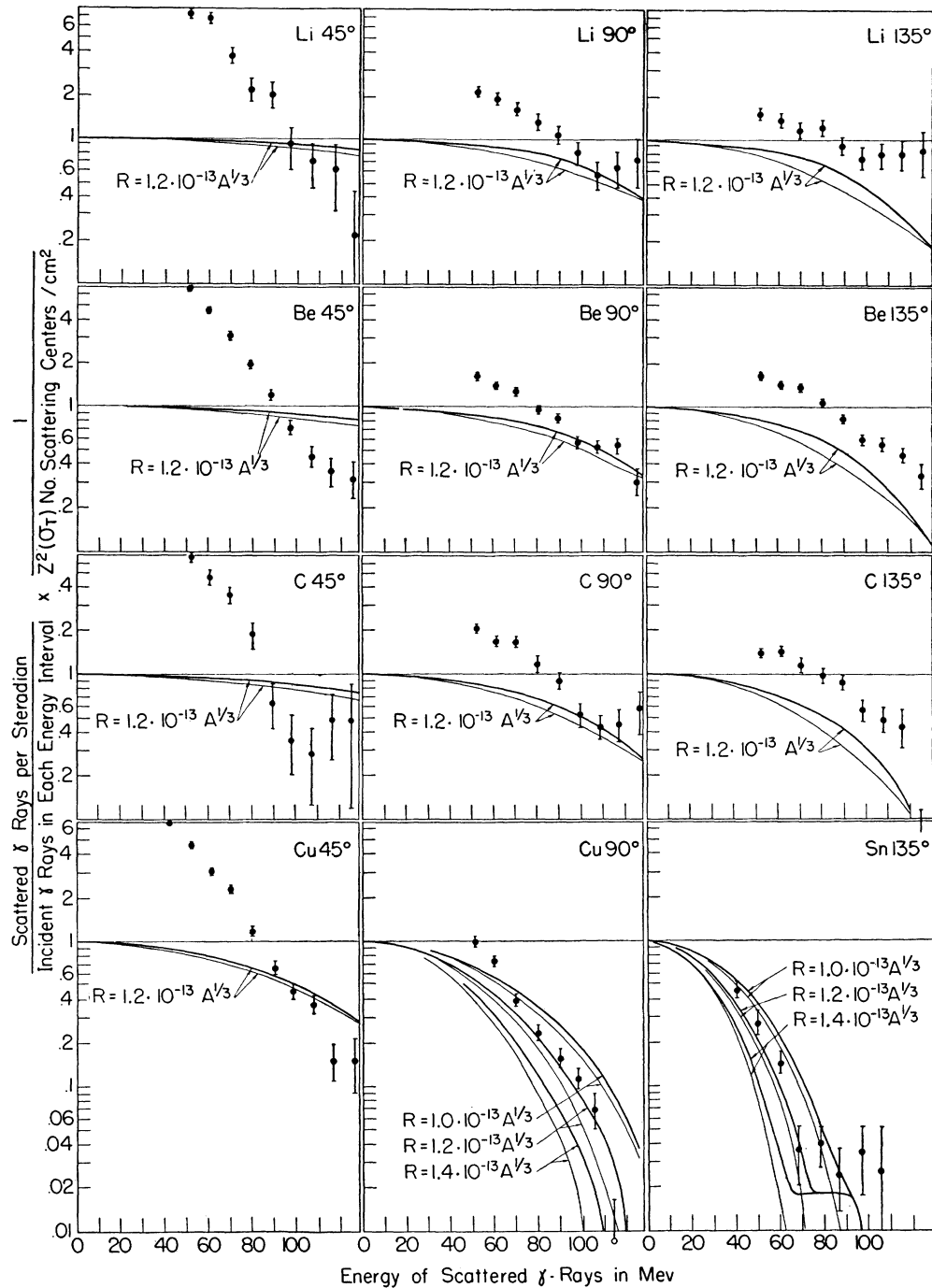


FIG. 5. Data on complex elements.

by Fuller and Hayward.<sup>10</sup> Because their highest energy point at 28 Mev has a large statistical error, the extrapolation to our lowest point at 40 Mev is very uncertain; but within the errors the two experiments agree.

The very large excess observed for low  $\gamma$ -ray energies at 45° appears to be in part of a very different origin, although it presumably contains the nuclear resonance

scattering as well. This effect was studied in several ways.

- (a) The yield was linear in target thickness.
- (b) The excess yield (above the yield found around 135°) was found to have a very steep angular dependence—roughly like  $\theta^{-4}$ . Figure 6(a) shows this angular dependence for two energy groups of  $\gamma$  rays.



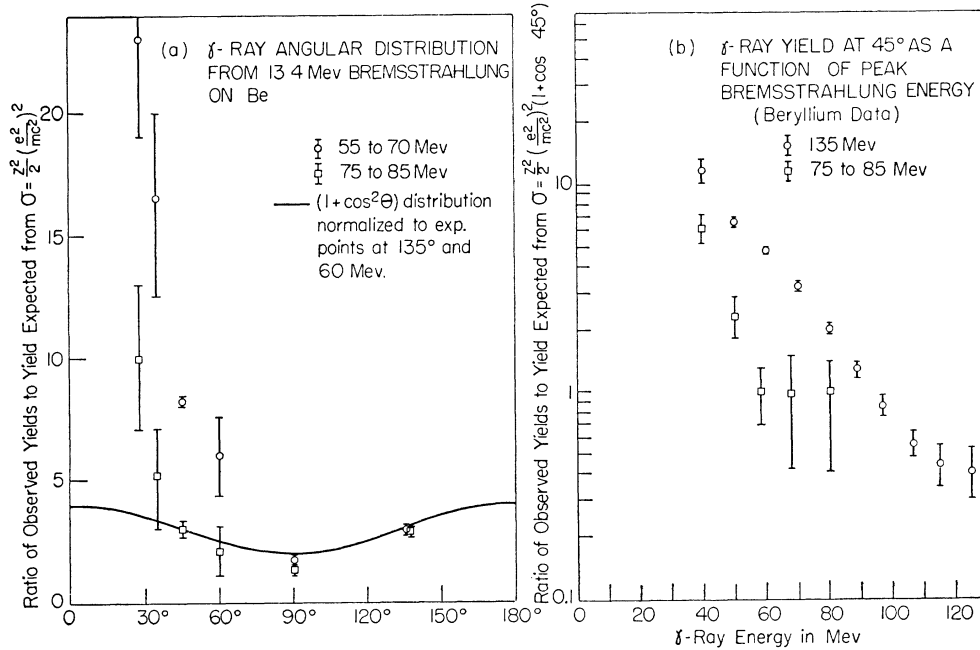


FIG. 6. (a) Angular dependence of low-energy  $\gamma$  rays. (b) Dependence of 45°  $\gamma$ -ray yield on peak beam energy.

(c) The low-energy yields were also studied as a function of peak energy of the bremsstrahlung beam to determine whether they represented elastic or inelastic processes. Figure 6(b) shows some results of this study when the peak energy was reduced to 80 Mev. It is clear that removal of high-energy photons in the incident beam decreased the yield of low-energy scattered photons. We conclude that much of the excess yield comes from an inelastic process.

(d) Finally in Fig. 5 it can be seen that at 45° these low-energy yields are very closely proportional to  $Z^2$ .

The behavior described above is consistent with the assumption that the  $\gamma$  rays resulted from radiative pair production—a higher order process in which one electron of the pair radiates a  $\gamma$  ray in the same Coulomb field in which it was produced. Since the process is proportional to  $Z^2$ , as is the Thomson cross section, one should expect to see this inelastic process just as clearly in the hydrogen data, Fig. 4 (c) and (d). Within the statistics (after correcting for the giant resonance in all elements except hydrogen), this seems to be the case.

## 2. 90 to 130 Mev

In the region from 90 to 130 Mev it seems likely that resonance effects from the complex nucleus are small, so the observed deviations from the modified Thomson yield are assumed to be effects of nucleon structure. In particular, these deviations are interpreted as a modification of the individual nucleon cross sections because of scattering associated with the virtual production of mesons. Experimentally, we find the most striking effect in light elements at 45°, for which the yields fall well below the modified Thomson values. There is also

an increase in the yield above the modified Thomson value at 135°. Figure 7(a) shows the data on beryllium plotted as a ratio to the modified Thomson value. The front-to-back asymmetry here is very clear. This effect can be simply interpreted as a result of interference between the Thomson electric dipole amplitude and a magnetic dipole amplitude associated with meson production. This effect is similar to what was observed with hydrogen. One expects the effect to be more pronounced in complex nuclei because both neutrons and protons can contribute to the meson-associated scattering while only the protons contribute to the Thomson component.

It would be interesting to determine whether this front-to-back asymmetry persisted in heavier elements. Unfortunately, the form factor for backward scattering by elements much heavier than carbon is so small that no useful data could be obtained. The form factor at 45°, however, is still quite close to unity even for copper. We therefore took a long run at 45° on copper. The data (Figs. 5) are not conclusive but suggest that the forward cross section is still low.

Figures 5 also show a long run on copper at 90°. This run was undertaken in the hope that we might be able to obtain an independent determination of the electromagnetic radius. The 90° angle was chosen because it was found that in light elements the deviation from the Thomson cross section due to mesonic effects was small at this angle. Copper was chosen because at 90° the nuclear size of copper makes the scattering a sharp function of radius for our particular wavelength of  $\gamma$  rays. There is no indication that the data are in disagreement with other determinations giving an effective radius of  $1.24 \frac{1}{2} \times 10^{-13}$  cm.

The run on Sn at 135° was taken to investigate nucleon-nucleon correlations in the complex nucleus. The cross section for inelastic scattering in this energy range can be sharply decreased below the predicted value if there are strong repulsive correlations in the motion of nucleons in the nucleus. On the other hand, the cross section would be increased if nuclei were composed of tightly bound sub-units. To make this test a nucleus whose form factor is almost zero at high energies was chosen. The remaining counts should then come from incoherent scattering. Before this run began, a routine target-out run was taken. However, in this run the total counting rate in the high-energy channels was so low that a really long target-out run should have been taken. This was not done, and so the slight excess of counts above the predicted value in the high-energy channels should not be taken too seriously. Furthermore, this is a case where the uncertainties inherent in the prediction of the inelastic scattering are very important.

IV. THEORY AND DISCUSSION

A. Nonpolarizable Nucleon Approximation

1. Scattering by a Free Proton

The Klein-Nishina and Powell<sup>15</sup> cross sections for the energy region of interest here are plotted in Fig. 8. Powell's calculation should give the most reliable estimate of scattering by a nonpolarizable proton. His calculation uses the Dirac Hamiltonian with a term for a point anomalous magnetic moment added. At our collision momenta the form factor for this anomalous moment should be almost unity. According to the Stanford electron-scattering data,<sup>17</sup> the over-all form factor for the proton should never be less than 0.93 in this experiment.

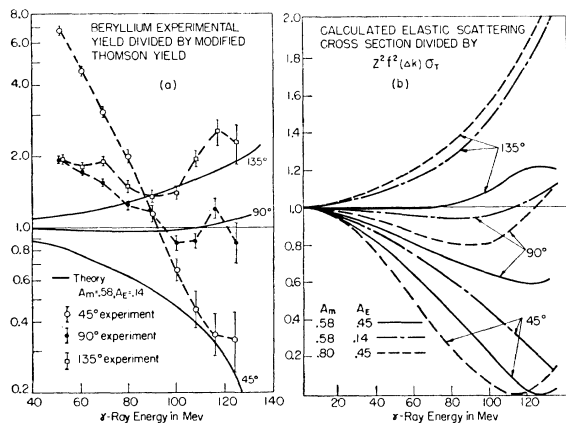


FIG. 7. Comparison of data on beryllium with theoretical results obtainable from dispersion theory on the assumption that a complex nucleus behaves as  $A$  free nucleons. Numerical values of  $A_M$  and  $A_E$  are given at meson threshold.

<sup>17</sup> R. W. McAllister and R. Hofstadter, Phys. Rev. **102**, 851 (1956).

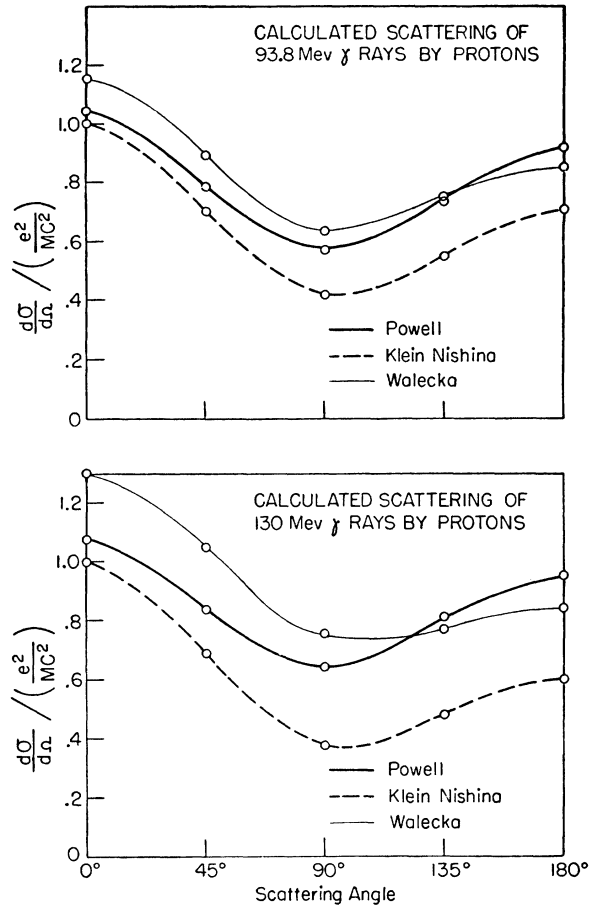


FIG. 8. Calculated  $\gamma$ -ray scattering by nonpolarizable protons.

2. Scattering by Complex Nuclei

In Sec. III we compared the elastic scattering from complex nuclei with the Thomson cross section for  $Z$  free protons, appropriately modified by a form factor. Use of this modified Thomson value as the expected cross section involved two assumptions (apart from the mesonic polarizability of the nucleons).

(a) The protons can be treated as free in the intermediate state for energies above about 85 Mev.

(b) Despite the anomalous magnetic moment and the large recoil of the protons in the intermediate states, the coherent scattering amplitude is approximately pure Thomson (again apart from mesonic polarizability).

We have no theoretical justification for the first assumption. However, the fact that the excess scattering at low energies approaches the modified Thomson limit quite rapidly in the 50- to 80-Mev region suggests that interaction with the complex nucleus is not very important above 80 Mev. In the theoretical treatment<sup>2</sup> this allows us to use second-order perturbation theory with unperturbed plane waves in the intermediate states, i.e., the impulse approximation. We thus neglect

processes in which protons are scattered in an intermediate state. We get the usual form factor  $f^2(\Delta k \cdot R)$  as a measure of the probability that the momentum of the proton can be absorbed in a return to the initial state wave function. (The final state is the same as the initial state for coherent scattering.)

For the atomic case, Brown and Woodward<sup>18</sup> found this approximation valid, provided  $f^2$  is not very small compared with unity. In this experiment  $f^2_{\text{Be}}(45^\circ, 130 \text{ Mev}) = 0.80$ , and  $f^2_{\text{Be}}(135^\circ, 130 \text{ Mev}) = 0.12$ .

The second assumption is in agreement with the result of a second order perturbation calculation carried out by one of the authors<sup>2</sup> using the Dirac Hamiltonian with the Pauli anomalous moment term added. For all nuclei in which the sum of the nucleon spins is zero, it was found that the Thomson cross section multiplied by the simple form factor  $f^2$  is exactly correct up to and including terms of order  $(p/Mc)^2$  and  $(k/Mc)^2$  (where  $p$  is the momentum of the nucleon in the nucleus, and  $k$  is the momentum of the  $\gamma$  ray). For other nuclei where spins do not cancel, one cannot neglect terms containing  $\sigma$ . An upper limit placed on these terms indicates that they do not exceed the fraction  $(\lambda k/ZMc)^2$  times the Thomson cross section. Even for Be this fraction is only about 10%. Thus the enhancement by coherence of the spin-independent part of the single-particle scattering amplitude makes Thomson scattering the major part of nuclear scattering, even though the anomalous moment causes the free-particle cross section to differ appreciably from the Thomson cross section at these energies.

## B. Nucleon Polarizability

### 1. Classical Calculation

One can get a qualitative picture of the scattering anomaly near meson threshold from a purely classical point of view. It is well known that nucleons can absorb  $\gamma$  rays through both magnetic dipole or electric dipole absorption. It follows that, if the nucleons have the necessary polarizability for absorption, they must also be able to scatter.

The case of the magnetic-dipole scattering is particularly clear. The absorption passes through a particular resonant state. Since both the maximum cross section and the energy width of this state have been measured, the resonance is completely determined, and one can predict the magnetic-dipole scattering amplitude as a function of energy. The value of the amplitude obtained in this way is in qualitative agreement with experiment. This magnetic-dipole scattering will interfere with the Thomson amplitude, which is electric dipole. The pattern of magnetic-dipole scattering is identical with electric-dipole scattering except that the role of the electric and magnetic vectors are interchanged. In the forward direction the amplitudes will

<sup>18</sup> G. E. Brown and J. B. Woodward, Proc. Roy. Soc. (London) **A65**, 977 (1952).

subtract because the magnetic-dipole scattering results from the low-energy tail of a resonance dispersion curve while the Thomson scattering is the free-particle limit and is phased like the high-energy tail of a dispersion curve. (See Fig. 9.) Likewise there is reinforcement in the backward direction.

If the electric-dipole meson production is associated with a simple electric polarizability of the meson-nucleon system (which seems compatible with the usual interpretation of photomeson observations), then the electric-dipole phase is also determined and will subtract from the Thomson amplitude at all angles. It is harder to make a good model for the electric-dipole scattering because no definite resonance appears to be involved. However, the classical dispersion relation can be used to obtain an estimate of the electric dipole amplitude.

If we normalize the Thomson scattering amplitude to 1 and let  $A_M$  be the magnetic dipole amplitude and  $A_E$  be the electric dipole amplitude, then we obtain an angular distribution given by

$$d\sigma/d\Omega = [(1 - A_E)^2 + A_M^2](1 + \cos^2\theta) - 4A_M(1 - A_E) \cos\theta.$$

According to this simple model of polarizable nucleons, one could account for scattering by complex nuclei simply by including the anomalous amplitudes from the neutrons in a coherent addition of amplitudes. Because of charge independence these should be the same as the corresponding amplitudes from the proton. Since there is no Thomson scattering by neutrons, one would then expect the ratio of the anomalous amplitudes to the Thomson amplitude to be about twice as great for complex nuclei as for hydrogen.

### 2. Quantum Calculation

Feld<sup>19</sup> has carried out a nonrelativistic calculation for protons which is the quantum equivalent of our classical interpretation of the magnetic-dipole scattering. Using the same matrix elements and wave functions which account satisfactorily for meson production, he has calculated that part of the scattering which goes through the  $T = \frac{3}{2}$ ,  $S = \frac{3}{2}$  state of the proton-meson system. He obtains about the same size anomaly with the same qualitative features, but his angular distribution for the non-spin-flip part is given by

$$d\sigma/d\Omega = [1 + (5/4)A_M^2](1 + \cos^2\theta) - 4A_M \cos\theta.$$

This differs from the classical result only in that  $A_M^2$  has been replaced by  $(5/4)A_M^2$ . The Feld calculation also obtains a spin-flip portion of the polarization scattering which is given by

$$d\sigma/d\Omega = \frac{1}{2}A_M^2 \sin^2\theta.$$

This term does not exceed 3% of the Thomson cross section below meson threshold. To our accuracy it can be ignored.

<sup>19</sup> B. T. Feld (private communication).

No such calculation has been made for the electric dipole amplitudes.

In order to combine any theoretical information on polarization scattering amplitudes with calculated scattering by nonpolarizable nucleons, it is, of course, necessary to know the phase of all the amplitudes involved. Unfortunately, this information is not contained in the Powell calculation. A more detailed discussion of this problem is given in the next section.

### C. Dispersion Relation

The recent quantum formulation of the dispersion relation enables one to predict the forward scattering amplitude if the total  $\gamma$ -ray absorption cross section is known as a function of energy. This technique has several applications to the present experiment.

#### 1. Application to Proton Scattering

Gell-Mann and Goldberger<sup>3,16</sup> have used the dispersion relations to predict the forward cross section for hydrogen and, using specific models, have estimated the cross section as a function of angle. They find that the forward-scattering amplitude  $f(\nu)$  is given by:

$$f(\nu) = f_1(\nu)\mathbf{e}' \cdot \mathbf{e} + f_2(\nu)i\boldsymbol{\sigma} \cdot (\mathbf{e}' \times \mathbf{e}),$$

where

$$f_1(\nu) = A_0 + \frac{\nu^2}{2\pi^2c} \int_0^\infty \frac{d\nu' \sigma(\nu')}{\nu'^2 - \nu^2 - i\epsilon},$$

and

$$f_2(\nu) = A_1\nu + \frac{\nu^3}{2\pi^2c} \int_0^\infty \frac{d\nu' \tilde{\sigma}(\nu')}{\nu'(\nu'^2 - \nu^2 - i\epsilon)}.$$

$f_1(\nu)$  is that part of the forward scattering amplitude which corresponds to the classical Kramers-Kronig<sup>20,21</sup> dispersion relation, and the  $\sigma(\nu)$  it contains is just the total  $\gamma$ -ray absorption cross section.  $f_2(\nu)$  contains  $A_1\nu$ , which represents scattering by the anomalous magnetic dipole. However,  $\tilde{\sigma}$  is not a simple cross section but is given by  $\tilde{\sigma} = \frac{1}{2}(\sigma_p - \sigma_a)$ , where  $\sigma_p$  is the absorption cross section for circularly polarized photons with spin parallel to the nucleon spin and  $\sigma_a$  is the corresponding cross section for the antiparallel case. Below meson threshold there is very little contribution from  $f_2(\nu)$  except from the term  $A_1\nu$ . Using averaged data from Cornell University, Massachusetts Institute of Technology, California Institute of Technology, and University of Illinois, we obtain slightly smaller values for the integral in  $f_1(\nu)$  than are given by Gell-Mann *et al.* At meson threshold we obtain  $f_1(\nu)/A_0 = 0.45$ , i.e., a forward-scattering intensity  $(0.45)^2$  times the Thomson value.

We would like to use the dispersion relation to obtain a theoretical estimate of the proton scattering as a

<sup>20</sup> R. Kamers, Atti. Congr. Intern. Fisici 2, 545 (1927).

<sup>21</sup> R. Kronig, J. Opt. Soc. Am. 12, 547 (1926).

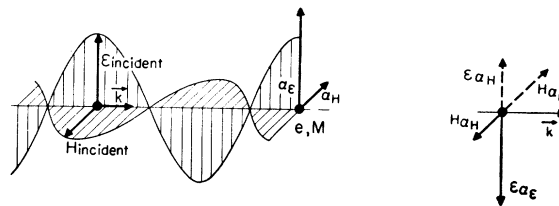


FIG. 9. Destructive interference of Thomson and magnetic polarization scattering in the forward direction. An electromagnetic wave is incident from the left on a proton of charge  $e$  and mass  $M$ . The electric field causes an acceleration  $\alpha_e$  in phase with the incident  $\mathcal{E}$  (since the proton is free). The magnetic field induces a magnetic moment, which is equivalent to accelerating a magnetic charge with  $\alpha_H$ . The phase of  $\alpha_H$  is  $180^\circ$  different from that of the incident  $H$ , since the magnetic-dipole resonance corresponding to the excited state of the proton occurs at a much higher frequency. The fields radiated in the forward direction are shown on the right, with phases corresponding to a distance from the proton of an integral number of wavelengths. The interference is destructive in the forward direction and constructive in the backward direction.

function of angle. The recoil is small in our energy region, so we will use the nonrelativistic approximation and evaluate separately the contribution to  $f_1(\nu)$  from the various multipoles taken in the center-of-mass system. The integral can be computed for each multipole separately according to its contribution in meson production. Thus  $f_1(\nu)$  will be broken into several parts, and we will have

$$f_1(\nu)/A_0 = 1 - A_E(\nu) - A_M(\nu),$$

where  $A_E(\nu)$  and  $A_M(\nu)$  are the anomalous electric and magnetic scattering amplitudes. At threshold, for example, we obtain  $A_E = 0.23$  and  $A_M = 0.29$ . The contribution from higher multipoles appears to be negligible. [Note added in proof.—It has been pointed out to us by F. Low that our separate evaluation of  $A_M$  and  $A_E$  from the causality relations is not strictly correct. We note, however, that the value  $A_M = 0.29$  thus obtained agrees, within the inaccuracy of application to our data, with the very approximate value  $A_M = 0.24$  obtained from Feld's expression.<sup>19</sup>]

Now we wish to use these quantities to modify the Powell calculation. To do this we must know the phase of the various parts of the Powell cross section. D. Walecka has begun a calculation which should yield this information, and has already completed a calculation using the nonrelativistic interaction Hamiltonian

$$H_{\text{int}} = \frac{-e}{M_{PC}} \mathbf{P} \cdot \mathbf{A} + \frac{e^2}{2M_{PC}^2} \mathbf{A}^2 - \lambda_p \frac{e\hbar}{2M_{PC}} \boldsymbol{\sigma} \cdot (\nabla \times \mathbf{A})$$

with relativistic kinematics. The resultant cross section (see Fig. 8) is about 20% higher than the Powell values at 130 Mev, showing that the nonrelativistic approximation is quite inadequate. However, we will try to use the calculation as a guide to the phases in the Powell cross section. Walecka's calculation gave an in-phase

part

$$d\sigma = \frac{1}{2} \left( \frac{e^2}{M_P c^2} \right)^2 \frac{k^2}{k_0^2} (1 + \cos^2\theta) d\Omega,$$

which is the dominant term in the Klein-Nishina formula at these energies. All important terms involving the magnetic moment were either spin-flip or  $90^\circ$  out of phase. Analogously, the Powell calculation gives the Klein-Nishina cross section plus terms in the anomalous magnetic moment. We will therefore assume that  $\sigma_{KN}$  is the in-phase component of the Powell cross section, which is to be interfered with our anomalous amplitudes  $A_E$  and  $A_M$ , and that the remaining terms are either spin-flip or out of phase so that their cross section, the excess above  $\sigma_{KN}$ , can simply be added to the result. This procedure gives us the curves shown in Fig. 4 (a), (b), (c) which are labeled "Powell+Dispersion." If one lets  $\lambda = -1$  in the Powell formula, corresponding to a particle with no net magnetic moment, one obtains a cross section<sup>22</sup> which, in our energy range, is almost identical with the Klein-Nishina formula. This result suggests that the identification of the Klein-Nishina cross section as the zero-moment case is not a serious error. For an accurate calculation one would, of course, separate the Powell calculation into in-phase and out-of-phase parts of both the spin-flip and non-spin-flip scattering. [Note added in proof.—R. Gomez and D. Walecka (Phys. Rev., to be published) have completed the exact breakup of the Powell cross section.] We avoid doing this because we ignore polarization contributions to the spin-flip and out-of-phase components.

It may be noted for the application of the dispersion relations that the Powell calculation makes no correction to the amplitude at  $0^\circ$ , except one linear in  $\nu$  which can be identified with  $A_1$ .

## 2. Application to Complex Nuclei

The application of the dispersion relation to complex nuclei is much more direct since we have shown that almost all the observed scattering is Thomson-like coherent scattering which has the same phase as  $f_1(\nu)$ . Unfortunately, the total absorption cross section is not adequately known. If, for the photon absorption cross section, we take the total meson production from a proton and multiply by the atomic mass number to include all neutrons and protons in the nucleus, we obtain approximately  $A_E = 0.45$ ,  $A_M = 0.58$ , where the coherent Thomson amplitude is taken as one. The resulting distribution (solid lines) is plotted in Fig. 7(b). This clearly predicts too little scattering at  $90^\circ$  and  $135^\circ$ . The situation can be improved either by decreasing  $A_E$  [the dashed lines, also plotted as "theory" in Fig. 7(a)] or increasing  $A_M$  (the dotted lines).

<sup>22</sup> S. B. Batdorf and R. Thomas, Phys. Rev. **59**, 621 (1941).

It would not be surprising if the  $A_E$  per nucleon were reduced in complex nuclei. The computed value of  $A_E$  receives a large contribution from the low-energy  $S$ -wave meson production, which is well known to be suppressed in complex nuclei.

Similarly, it would not be surprising if the  $A_M$  per nucleon were increased in complex nuclei because the  $A_M$  receives its main contribution from a region well above threshold, and coherent meson production could give rise to an increase in the total absorption cross section.

## D. Relation to Antiproton Scattering

Our interpretation of the data for complex nuclei has been based on neglect of nuclear interactions in the intermediate states, at least when the form factor is not too small. In the perturbation treatment, the Thomson scattering occurs primarily through virtual transitions to the negative energy states, equivalent to considering antiprotons to exist in the intermediate states.

On the other hand, there is now some evidence for exceptionally strong interactions of antiprotons with nuclear matter. A more quantitative interpretation of  $\gamma$ -ray scattering data in this energy region might yield information on the interaction of antiprotons within nuclei.

## E. Relation to Electron Scattering

The information obtained in  $\gamma$ -ray scattering is quite different from the information obtained in elastic electron scattering.<sup>23,24</sup> The electron scattering measures almost exclusively the properties of the ground state of the scatterer; the  $\gamma$ -ray scattering is sensitive to both ground state and the excited states.

In lowest order, electron scattering may be described as the emission of a single quantum by one charged particle and its absorption by the other. In order to involve an excited state of one of the scatterers, a two-quantum process must occur. This is much less probable than the one-quantum process. Furthermore, the quanta in the two-quantum process have a continuous spectrum of energies, and the amplitudes from the two sides of the resonance almost cancel out because they have opposite phase. A calculation by Drell and Ruderman<sup>25</sup> shows that this cancellation is extremely effective, so that resonances are not likely to produce more than a 0.1% effect in electron scattering.

In  $\gamma$ -ray scattering the two quanta have a unique energy, and the process is consequently very sensitive to resonant structure.

<sup>23</sup> J. H. Fregau and R. Hofstadter, Phys. Rev. **99**, 1503 (1955).  
<sup>24</sup> Holm, Ravenhall, and Hofstadter, Phys. Rev. **101**, 1131 (1956).

<sup>25</sup> S. D. Drell and M. A. Ruderman (to be published).

## V. ACKNOWLEDGMENTS

The authors wish to express their appreciation to L. S. Osborne for the initial suggestion of this experiment, and to him, S. D. Drell, B. T. Feld, F. Villars, A. Wattenberg, and V. F. Weisskopf for many ideas,

calculations, and discussions. We are also very much indebted to D. Walecka for several difficult computations, to J. L. Powell for sending us the details of his calculation, and to B. Richter and J. Russell for help in running the experiment.

## Energies of Nuclei with Different Proton and Neutron Shells

S. GOLDSTEIN AND I. TALMI\*

*Department of Physics, The Weizmann Institute of Science, Rehovoth, Israel*

(Received October 31, 1956)

Analysis of energies of nuclei in which protons and neutrons occupy different unfilled shells is made on the basis of the shell model. Good agreement of the calculated and experimental energies is obtained in the  $s_{1/2}d_{3/2}$  and the  $d_{3/2}f_{7/2}$  regions. Parameters characterizing the nuclear interaction were determined. When these are used in the case of  $K^{42}$  the right spin is obtained for the ground state.

## I. INTRODUCTION

RECENTLY<sup>1</sup> binding energies of nuclei were calculated on the basis of the shell model. In all the nuclei treated in this reference, the protons and the neutrons occupy the same unfilled shell. Thus, group theoretical methods could be used which simplified the calculation. In the present paper we deal with nuclei where the unfilled proton shell is different from the neutron unfilled shell. The same approach of reference 1 is used also here. We investigate to what extent we can use the simple shell model in the calculation of energy levels. We first assume that the wave function of the nucleus is that of nucleons moving independently in a central field (the form of which is not specified); the total spin of each nucleon is a good quantum number ( $jj$ -coupling shell model wave function). We further assume that the potential energy of the system comes from a mutual interaction of the nucleons which is a general (unspecified) two body force.

Obviously, this is not sufficient to carry out a mathematical evaluation of the energies. The first assumption fixes only the angular and spin part of the wave functions but nothing is assumed on the radial functions of the single nucleons. Moreover, the interaction of free nucleons is not very well known and it is certainly not known what interaction should be considered in shell model calculations. Therefore, in order to overcome this difficulty, we do not make any specific assumption on the two-body interaction (which might be an arbitrary mixture of various central forces, mutual spin-orbit interactions, and tensor forces as well as other possible velocity-dependent interactions).

The situation is analogous to that in atomic spectroscopy. Although the interaction in that case is well known (the electrostatic repulsion of the electrons), the radial part of the wave functions is rather difficult to calculate. The usual procedure is to express the energy levels of a certain atom in terms of a number of parameters. These are various radial integrals of the Coulomb potential (Slater integrals). Usually, the number of levels is much bigger than the number of parameters. Therefore, a criterion to the validity of the theory (the configuration assignment, the coupling scheme, etc.) is whether values of the parameters can be found which satisfactorily reproduce the observed levels. Such values are usually determined by a least-squares fit.

We use the same procedure also in the case of nuclear spectra. However, unlike the atomic case, only a few nuclear levels are definitely assigned a certain configuration. Therefore, there are usually more parameters than experimental data of a single nucleus. We can apply the method described above only if we take into consideration a group of several nuclei, thereby increasing the number of data. In order to do this we have to postulate the way the parameters change in going from one nucleus to another. In the following we assume that the parameters are the same for the group of all nuclei in which the same shells are being filled. This means that the potential well which determines the single-nucleon wave functions is the same for all nuclei in one group. This assumption as well as the previous ones have been justified by previous results<sup>1,2</sup> and by the results of the present work. This behavior of the parameters should be contrasted with the atomic case where the parameters change appreciably on going from one atom to the next. In most nuclei only the ground state can be assigned by the shell model a definite configuration. In order to

\* On leave of absence at the Palmer Physical Laboratory, Princeton University, Princeton, New Jersey, during the academic year 1956-1957.

<sup>1</sup> I. Talmi and R. Thieberger, Phys. Rev. **103**, 718 (1956).

<sup>2</sup> S. Goldstein and I. Talmi, Phys. Rev. **102**, 589 (1956).